

University of Nebraska - Lincoln

## DigitalCommons@University of Nebraska - Lincoln

---

Stephen Ducharme Publications

Research Papers in Physics and Astronomy

---

August 2005

### Manifestation of a Ferroelectric Phase Transition

A. R. Geivandov

*Shubnikov Institute of Crystallography, Russian Academy of Sciences, Moscow, Russia*

S.G. Yudin

*Shubnikov Institute of Crystallography, Russian Academy of Sciences, Moscow, Russia*

V.M. Fridkin

*Shubnikov Institute of Crystallography, Russian Academy of Sciences, Moscow, Russia*

Stephen Ducharme

*University of Nebraska, [sducharme1@unl.edu](mailto:sducharme1@unl.edu)*

Follow this and additional works at: <https://digitalcommons.unl.edu/physicsducharme>

 Part of the [Physics Commons](#)

---

Geivandov, A. R. ; Yudin, S.G.; Fridkin, V.M.; and Ducharme, Stephen, "Manifestation of a Ferroelectric Phase Transition" (2005). *Stephen Ducharme Publications*. 2.

<https://digitalcommons.unl.edu/physicsducharme/2>

This Article is brought to you for free and open access by the Research Papers in Physics and Astronomy at DigitalCommons@University of Nebraska - Lincoln. It has been accepted for inclusion in Stephen Ducharme Publications by an authorized administrator of DigitalCommons@University of Nebraska - Lincoln.

---

## MAGNETISM AND FERROELECTRICITY

---

# Manifestation of a Ferroelectric Phase Transition in Ultrathin Films of Polyvinylidene Fluoride

A. R. Geĭvandov\*, S. G. Yudin\*, V. M. Fridkin\*, and S. Ducharme\*\*

\*Shubnikov Institute of Crystallography, Russian Academy of Sciences, Leninskii pr. 59, Moscow, 119333 Russia  
e-mail: LBF@ns.crys.ras.ru

\*\*University of Nebraska, Lincoln, USA

Received October 5, 2004

**Abstract**—Temperature dependences of the dielectric properties of ultrathin polyvinylidene fluoride films prepared using the Langmuir–Blodgett method were studied by linear and nonlinear dielectric spectroscopy. It is shown that ultrathin Langmuir films of polyvinylidene fluoride exhibit a manifestation of a first-order ferroelectric phase transition, which can be assigned to the interaction between the spontaneous polarization and the surfaces bounding the film. As the film thickness increases, the effect of the surfaces decreases and the ferroelectric phase transition shifts to high temperatures to vanish altogether when the temperature region of the transition rises above the melting point. © 2005 Pleiades Publishing, Inc.

### 1. INTRODUCTION

Numerous experimental studies seem to suggest that observation of the ferroelectric phase transition in polyvinylidene fluoride (PVDF) is impossible because bulk samples (films with a thickness of above 100 nm) undergo melting before the onset of the hypothetical transition to the ferroelectric phase [1–3]. It was shown in [4] that, as one crosses over to ultrathin (less than 5-nm-thick) Langmuir–Blodgett (LB) films [5] of 70/30 vinylidene fluoride copolymer with trifluoroethylene (VDF/TrFE), the ferroelectric phase transition region shifts toward lower temperatures. It is known [3, 4] that films of pure PVDF have a lower spontaneous polarization than copolymer films (such as VDF/TrFE). This can be accounted for by the low crystallinity of PVDF films (the content of the ferroelectric  $\beta$  phase is approximately 50%). We believe that the effect of the bounding surfaces on the sample properties increases with decreasing PVDF film thickness. The fact is that surface layers of a ferroelectric behave differently from the bulk of the material. Because boundary layers of thin films contribute more to the sample characteristics under study than those of thick films, the properties of the sample on the whole change. Thus, it is thin films that offer the possibility of studying the ferroelectric phase transition in films prepared of pure PVDF. Note that the ferroelectric phase transition has been observed previously only in copolymers (such as VDF/TrFE) of different compositions (from 37/63 to 73/27) [2–4].

The present paper reports on a study of the temperature dependences of the dielectric properties of PVDF ferroelectric films prepared using the LB method by linear and nonlinear dielectric spectroscopy (NDS).

### 2. SAMPLE PREPARATION AND EXPERIMENT

The PVDF molecule consists of  $(-\text{CH}_2-\text{CF}_2-)$  monomer chain links. The total molecular mass of the polymer chain is approximately  $10^5$ . LB films of PVDF were obtained in a setup described in [6]. First, a solution of 0.01–0.02 wt % PVDF in acetone was prepared. PVDF monolayers were transported from the water surface, using the Langmuir–Schaffer method [5] (horizontal lifting), onto glass substrates with 1-mm-wide aluminum electrodes evaporated in vacuum. The PVDF films were deposited under a surface pressure  $\pi = 1.5\text{--}3$  mN/m at a temperature of 17–19°C. The number of layers (from 5 to 36) was varied depending on the desired total film thickness. The thickness of one monolayer as estimated from the size of the PVDF molecule is 0.5 nm [4]. It is known, however, that the thickness of a film after its deposition on the substrate turns out to be larger. Indeed, as follows from capacitance measurements, the thickness of one transported layer exceeds the calculated value by two to three times [7]. After the layer deposition, a top aluminum electrode was evaporated such that the electrode overlap area was  $1 \pm 0.0025$  mm<sup>2</sup>.

The electric properties of LB PVDF films were measured on an automated setup. A computer audio card was used to generate and detect electric signals. The measurement system consisted of a set of virtual instruments (a generator, a lock-in detector, a digital oscilloscope, etc.) realized with the PhysLab computer code [6]. The setup included a thermostat, whose temperature was monitored by means of a Peltier element and measured with a platinum resistance thermometer. The sample temperature was varied from 30 to 185°C.

The dielectric properties of LB PVDF films were studied by NDS, the principles of which are explained in detail in [8, 9].

The NDS method is based on phase-sensitive measurements of the fundamental and higher harmonics of the current flowing through a sample to which a harmonic voltage is applied. Therefore, lock-in detection was employed for current measurement [8]. In this method, the sample, which can generally be considered a capacitance and a resistance connected in parallel, is inserted in series with a load resistor and the voltage drop across it (which is proportional to current) is measured by the detector. The reference signal for lock-in detection is supplied from a second generator channel.

When a sine voltage  $U(t) = U_0 \sin(\omega t)$  is applied to a sample, the total current in the measuring electric circuit is given by

$$I = \frac{U_0 \sin \omega t}{R} + \omega U_0 C_0 \cos(\omega t) + \omega U_0^2 \sin(2\omega t) \frac{dC}{dU}, \quad (1)$$

where  $\omega = 2\pi f$  is the circular frequency,  $U_0$  is the amplitude of the voltage  $U$  applied to the sample,  $t$  is the time, and  $f$  is the frequency of the sine voltage. The first term is inversely proportional to the Ohmic resistance of the sample  $R$ . The second term is proportional to the sample capacitance  $C_0 = C(U = 0)$ . These terms are easily separated in lock-in detection, because they are shifted in phase by  $90^\circ$ . The third term is the nonlinear contribution connected with the ferroelectric properties of the sample under study.

Ferroelectricity can be conveniently studied by introducing quantities that are defined through the ratios of the Fourier components [8] measured by the lock-in detector. In the case where the fourth and the fifth current harmonics are negligible (at the noise level), the intermodulation contributions to the first three harmonics are small and we can write

$$A_2 = \frac{-\sqrt{2}\Phi_{2x}}{2\left(\sqrt{2}\Phi_{1y} - \omega\epsilon_0 \frac{U_0 S}{d}\right)^3} \frac{U_0}{d} (\omega S)^2, \quad (2)$$

$$A_3 = \frac{\sqrt{2}\Phi_{3y}}{3\left(\sqrt{2}\Phi_{1y} - \omega\epsilon_0 \frac{U_0 S}{d}\right)^4} \frac{U_0}{d} (\omega S)^3, \quad (3)$$

$$A_4 = \frac{\sqrt{2}\Phi_{4x}}{15\left(\sqrt{2}\Phi_{1y} - \omega\epsilon_0 \frac{U_0 S}{d}\right)^5} \frac{U_0}{d} (\omega S)^4, \quad (4)$$

$$A_5 = \frac{-2\sqrt{2}\Phi_{5y}}{5\left(\sqrt{2}\Phi_{1y} - \omega\epsilon_0 \frac{U_0 S}{d}\right)^6} \frac{U_0}{d} (\omega S)^5, \quad (5)$$

where  $S$  is the electrode overlap area;  $d$  is the film thickness;  $\epsilon_0 \cong 8.85 \times 10^{-12}$  F/m; and  $\Phi_{1y}$ ,  $\Phi_{2x}$ ,  $\Phi_{3y}$ ,  $\Phi_{4x}$ , and  $\Phi_{5y}$  are the effective values of the Fourier  $x$  and  $y$  components detected by the lock-in detector, from the first to the fifth harmonic. Recall that the  $x$  component should be identified with the signal that is in phase with the reference (which, in turn, is proportional to  $\sin(k\omega t)$ , where  $k$  is the harmonic number), whereas the  $y$  component is proportional to  $\cos(k\omega t)$  and, hence, is shifted with respect to the reference signal by  $90^\circ$ . The quantities  $A_k$  ( $k = 2, 3, 4, 5$ ) were obtained in the approximation of infinite sample resistances.

The convenience of using the above quantities becomes obvious when one learns their relation to the Landau–Ginzburg coefficients in the equation for the free energy of the ferroelectric [10]:

$$F_{LG} = \frac{1}{2}\alpha P^2 + \frac{1}{4}\beta P^4 + \frac{1}{6}\gamma P^6 - EP, \quad (6)$$

$$\alpha = \alpha_0(T - T_0),$$

where  $\alpha_0$ ,  $\beta$ , and  $\gamma$  are temperature-independent coefficients;  $T_0$  is the Curie temperature;  $E$  is the electric field amplitude; and  $P$  is the polarization. As shown in [8], quantities (2)–(5) for a uniformly polarized ferroelectric can be expressed as

$$A_2 = P_s(3\beta + 10\gamma P_s^2), \quad (7)$$

$$A_3 = \beta + 10\gamma P_s^2, \quad (8)$$

$$A_4 = \gamma P_s, \quad (9)$$

$$A_5 = \gamma, \quad (10)$$

where  $P_s$  is the spontaneous polarization.

We readily see that the quantity  $A_3$  is connected with the coefficient  $\beta$ , which, together with the coefficient  $\gamma$ , determines the order of the phase transition. It is known that, for  $\beta > 0$  and  $\gamma \geq 0$ , Eq. (6) describes a second-order phase transition and, for  $\beta < 0$  and  $\gamma > 0$ , the first-order transformation. Thus, in the case of a first-order phase transition, there is a temperature at which  $A_3$  can vanish and reverse sign.

In addition to NDS, polarization switching in films was probed using the classical Merz method [11], in which triangular voltage pulses are applied to a sample and the current response is measured as the voltage drop across the load resistor connected in series with the sample. In addition to the capacitive and resistive current contributions, the current response contains characteristic nonlinear contributions originating from switching of the spontaneous polarization (Fig. 1).

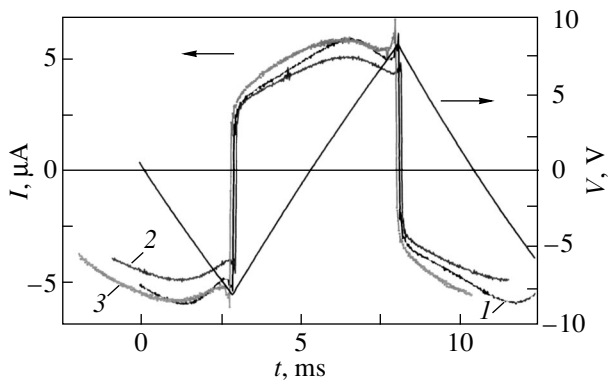


**Fig. 1.** Oscilloscopic traces of current (left) obtained with triangular voltage pulses of amplitude  $U_0 = 14$  V and frequency  $f = 96$  Hz applied to the sample at various temperatures  $T$ : (1) 35, (2) 57, and (3) 88°C.

### 3. DISCUSSION OF THE RESULTS

The LB PVDF films exhibit ferroelectric properties. This is borne out by observation of the characteristic current responses obtained using the Merz technique [11] (Fig. 1).

Figure 2 shows the temperature dependences of the first and third current harmonics. The thermal hysteresis seen in the permittivity of the 5-layer LB PVDF film (curve 1 in Fig. 2a) indicates a first-order phase transition similar to the one observed in LB films of a VDF/TrFE 70/30 copolymer [12]. However, the amplitude of the first current harmonic in the VDF/TrFE 70/30 copolymer films varied within a factor of 1.5 to 2 during heating and cooling runs, whereas the variation in this quantity in the 5-layer PVDF film does not exceed 10%. As the LB PVDF film thickness increases to 10 layers (curve 1 in Fig. 2b), the thermal hysteresis becomes less pronounced, with the maxima shifting toward higher temperatures. For instance, the maximum at 147°C (Fig. 2a, heating run) shifts to 160°C (Fig. 2b, heating) and the maximum at 108°C (Fig. 2a, cooling run) shifts to 119°C (Fig. 2b, cooling). A further increase in the LB PVDF film thickness to 36 layers entails a shift of the ferroelectric phase transition to high temperatures, where melting occurs and the transition becomes virtual. We explain these experimental data as due to the fact that the free-energy contribution generated by surface interaction becomes progressively more significant with decreasing film thickness than that due to the bulk of the sample. The low-temperature shift of the phase transition is caused by the polarization interacting with the surface. Because the surface interaction is localized, there occurs a surface-induced phase transition in thin surface layers. Thus, ultrathin films of pure PVDF exhibit a superposition of two ferroelectric phase transitions, more specifically, of a surface-induced and a bulk transition. The surface-induced phase transition is characterized by a Curie temperature lying below the melting point ( $T_m \approx 168$ – $170^\circ\text{C}$ ), while

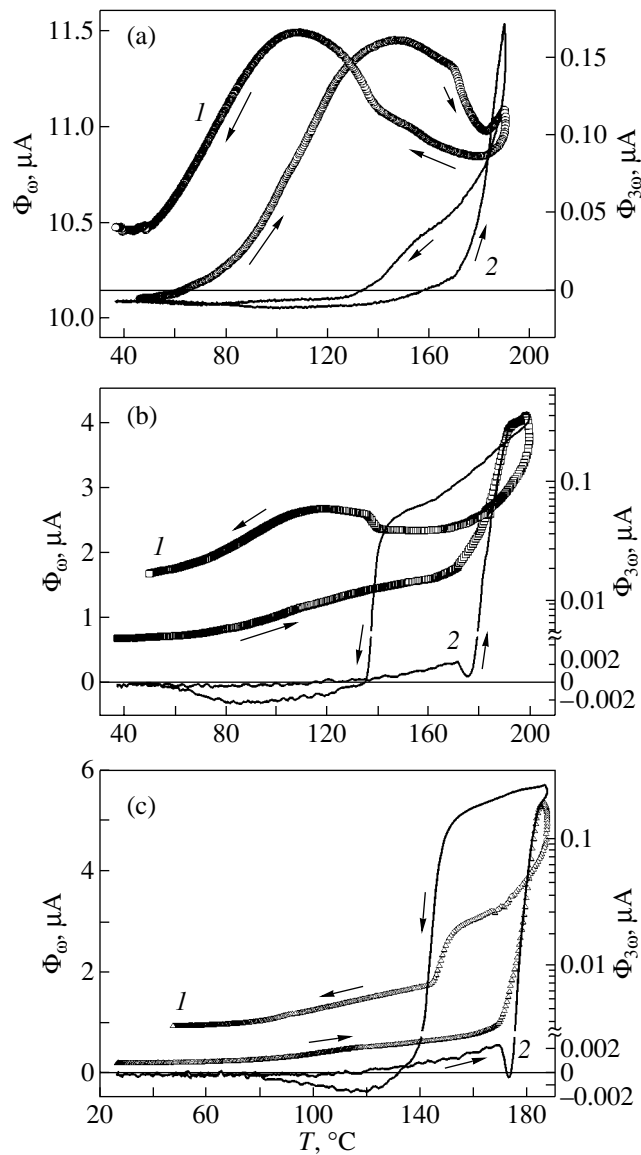


**Fig. 2.** Temperature dependences of (1) the fundamental and (2) third harmonics in the current for PVDF films with various thicknesses: (a) 5, (b) 10, and (c) 36 layers.  $U = 0.5$  V and  $f = 1$  kHz. Arrows refer to sample heating and cooling. The right-hand scale in panels (b, c) is linear near zero and logarithmic otherwise.

in bulk samples a ferroelectric phase transition cannot be observed, because it is expected to occur in the melting-temperature region, as indicated in a number of papers [1, 3].

The existence of a first-order phase transition is also corroborated by the clearly pronounced sign reversal of the third harmonic in the current response (curve 2 in Fig. 2a) observed at 156°C on heating and at 132°C on cooling, because, as follows from Eqs. (3) and (8), sign reversal is possible only for  $\beta < 0$ . In 10- and 36-layer-thick LB films, however, it becomes difficult to reliably detect sign reversal of the third harmonic (Figs. 2b, 2c)

during heating. At temperatures below 100°C, the signal is very low. Note that the right-hand scale in Figs. 2b and 2c is divided into a linear (near the zero signal) and a logarithmic (region of positive response) part. A distinct sign reversal in the vicinity of  $T = 132^\circ\text{C}$  in 10- and 36-layer films could be identified only in the cooling run. Thus, measurement of the third harmonic in the current response again reveals the above-mentioned interplay between the surface-induced and bulk ferroelectric phase transitions with increasing film thickness.

Figures 3a and 3b display the temperature dependences of  $A_3$  for 5- and 10-layer PVDF films, respectively. The quantity  $A_3$  is expressed through the first and third current harmonics and is a more revealing characteristic for describing the ferroelectric properties of a uniform sample [see Eqs. (3), (8)]. The condition  $A_3 = 0$  for a 5-layer film is met at  $156^\circ\text{C}$  (under heating) and at  $132^\circ\text{C}$  (under cooling). In the paraelectric phase, where  $P_s = 0$ , the quantity  $A_3$  is negative and temperature-independent, according to Eq. (8) for the uniform model. It has indeed been found that, in LB films of the VDF/TrFE 70/30 copolymer above the transition temperature  $T \cong 110^\circ\text{C}$ , the value of  $A_3$  in the paraelectric phase is negative and that the  $A_3(T)$  dependence is weak (the curve is parallel to the horizontal axis) and switches sign only on cooling to  $70^\circ\text{C}$  [8]. In our case, the 5-layer LB PVDF film (Fig. 3a) exhibits a weak  $A_3(T)$  dependence in the temperature regions 120–150°C (under heating) and 130–90°C (under cooling). Although  $A_3 > 0$ , we attribute these temperature regions to the paraelectric state of the surface layer of the film (surface-induced ferroelectric phase transition). The fact that  $A_3 > 0$  in these regions may be explained as being due to the positive background produced by the bulk of the film, which resides in the ferroelectric state. It is because of the dominant background due to the bulk of the film that analysis of the surface-induced ferroelectric phase transition is hampered (Fig. 3b). Thus, only in the 5-layer LB PVDF film does the  $A_3(T)$  dependence exhibit features characteristic of the surface-induced ferroelectric phase transition; these features are not manifest in thicker films.

The experimental data can be qualitatively treated in terms of the quasi-uniform model with inclusion of the nonpolar part of the surface energy. Using the approach explicated in [9], the nonpolar contribution to the surface energy can be found to be

$$W_2 = \frac{1}{2} W_{2m} (P_i n_{e,i})^2, \quad (11)$$

where  $W_{2m}$  is the surface energy amplitude,  $P_i$  are the components of the spontaneous polarization vector (the index  $i$  labels the spatial directions  $x, y, z$ ), and  $n_{e,i}$  are the components of the unit vector  $\mathbf{n}_e$  oriented along the specific (“easy”) direction on the surface. The concept of specific direction (easy axis) is introduced here by

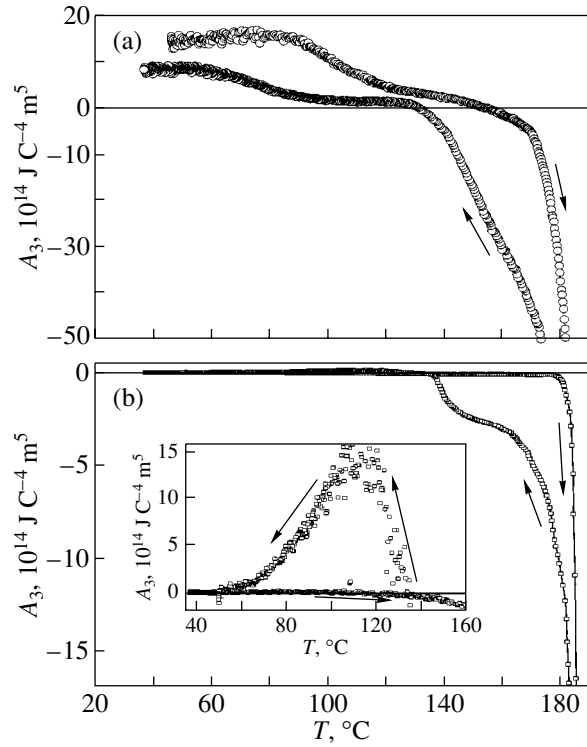


**Fig. 3.** Temperature dependences of the coefficient  $A_3$  for PVDF films (a) 5- and (b) 10-layers thick.  $U = 0.5$  V and  $f = 1$  kHz. Arrows refer to sample heating and cooling. In the inset, the coefficient  $A_3$  is shown in an enlarged scale.

analogy with the description of surface interaction (cohesion) in the theory of liquid crystals [13]. The easy axis corresponds to extremal values of surface interaction. For instance, in the particular case of an isotropic substrate surface, the only preferred direction is the surface normal  $\mathbf{n}_s$ , so  $\mathbf{n}_e = \mathbf{n}_s$ . Near the surface, there is always an electric field, and its spatial distribution is dependent on the symmetry properties of this surface. The surface energy quadratic in polarization reflects the nonpolar interaction of this field with the polarization.

Let us consider the free energy of a planar uniform ferroelectric domain, with the easy axis vector  $\mathbf{n}_e$  aligned with the surface normal  $\mathbf{n}_s$ . With inclusion of the nonpolar surface interaction, the free-energy density of a uniform ferroelectric can be written in the form

$$F = \frac{1}{2} \alpha P_z^2 + \frac{1}{4} \beta P_z^4 + \frac{1}{6} \gamma P_z^6 - E_z P_z - [W_{2m,s1} P_z^2 \delta(0) + W_{2m,s2} P_z^2 \delta(z-d)], \quad (12)$$

where  $P_z$  and  $E_z$  are the  $z$  components of the spontaneous polarization and electric field, respectively (the  $z$  axis is directed along the surface normal);  $\delta(z)$  is a delta function characterizing the localization of the surface interaction; and  $W_{2m,s1} P_z^2 \delta(0) + W_{2m,s2} P_z^2 \delta(z-d)$  is the

sum of the quadratic surface energies localized near the two surfaces of the  $d$ -thick film. Obviously enough, the sum of quadratic surface energies describing the non-polar interaction between the surface and the polarization vector  $P_z$  modifies the coefficient  $\alpha$ . The sign of this sum in Eq. (12) can be either positive or negative, depending on which (normal or planar) orientation of the polarization vector is preferred for a given surface. We chose the minus sign in order for the polarization orientation along the surface normal to be favorable at positive values of  $W_{2m}$ . Accordingly, the temperature of the surface-induced phase transition can either increase or decrease, depending on the sign of  $W_{2m}$ . Measurement of the dependence of the first Landau coefficient  $\alpha$  on film thickness in more uniform LB films of the VDF/TrFE 70/30 copolymer would make it possible to quantify the quadratic surface interaction.

#### 4. CONCLUSIONS

Using nonlinear dielectric spectroscopy, we have shown that, as the film thickness is reduced, a ferroelectric phase transition (which is absent in bulk samples) begins to appear. A qualitative theoretical model based on the Landau–Ginzburg theory with inclusion of surface interaction has been proposed for describing this surface-induced phase transition.

#### ACKNOWLEDGMENTS

The authors are indebted to S.P. Palto for his assistance in the study and helpful discussions.

This study was supported by the Russian Foundation for Basic Research (project nos. 03-02-17288, 04-02-16466), the International Association of European Communities (project no. 03-51-39-67), and the Department of Physical Sciences of the Russian Acad-

emy of Sciences (program “Novel Materials and Structures”).

#### REFERENCES

1. *The Applications of Ferroelectric Polymers*, Ed. by T. T. Wang, J. M. Herbert, and A. M. Glass (Chapman and Hall, New York, 1988).
2. K. Koga and H. Ohigashi, *J. Appl. Phys.* **59**, 2142 (1986).
3. T. Furukawa, M. Date, and E. Fukada, *Ferroelectrics* **57**, 63 (1980).
4. A. V. Bune, V. M. Fridkin, S. Ducharme, L. M. Blinov, S. P. Palto, A. V. Sorokin, S. G. Yudin, and A. T. Zlatkin, *Nature* **391**, 274 (1998).
5. J. Langmuir and V. Schaffer, *J. Chem. Soc.* **59**, 2400 (1937).
6. S. P. Palto, Doctoral Dissertation (Inst. Kristallogr. Ros. Akad. Nauk, Moscow, 1998).
7. L. M. Blinov, V. M. Fridkin, S. P. Palto, A. V. Bune, P. A. Dauben, and S. Dyusharm, *Usp. Fiz. Nauk* **170** (3), 247 (2000) [*Phys. Usp.* **43** (3), 243 (2000)].
8. S. P. Palto, G. N. Andreev, N. N. Petukhova, S. G. Yudin, and L. M. Blinov, *Zh. Éksp. Teor. Fiz.* **117** (5), 1003 (2000) [*JETP* **90** (5), 872 (2000)].
9. A. R. Geĭvandov, S. P. Palto, S. G. Yudin, and L. M. Blinov, *Zh. Éksp. Teor. Fiz.* **126** (1), 99 (2004) [*JETP* **99** (1), 83 (2004)].
10. V. L. Ginzburg, *Zh. Éksp. Teor. Fiz.* **19**, 36 (1949).
11. W. J. Merz, *J. Appl. Phys.* **27**, 938 (1956).
12. S. P. Palto, A. M. Lotonov, K. A. Verkhovskaya, G. N. Andreev, and N. D. Gavrilova, *Zh. Éksp. Teor. Fiz.* **117** (2), 342 (2000) [*JETP* **90** (2), 301 (2000)].
13. R. Barberi, I. Dozov, M. Giocondo, M. Iovane, Ph. Martinot-Lagarde, D. Stoenescu, S. Tonchev, and L. V. Tsonev, *Eur. Phys. J. B* **6**, 83 (1998).

*Translated by G. Skrebtsov*